

Transition from the Couette-Taylor system to the plane Couette system

Holger Faisst and Bruno Eckhardt

Fachbereich Physik, Philipps Universität Marburg, D-35032 Marburg, Germany

(Received 29 November 1999)

We discuss the flow between concentric rotating cylinders in the limit of large radii where the system approaches plane Couette flow. We discuss how in this limit the linear instability that leads to the formation of Taylor vortices is lost and how the character of the transition approaches that of planar shear flows. In particular, a parameter regime is identified where fractal distributions of lifetimes and spatiotemporal intermittency occur. Experiments in this regime should allow us to study the characteristics of shear flow turbulence in a closed flow geometry.

PACS number(s): 47.20.Lz, 47.27.Cn, 47.20.Ft

The transition to turbulence for a fluid between concentric rotating cylinders has attracted much experimental and theoretical attention. Ever since Taylor's success [1] in predicting and observing the instabilities for the formation of vortices the system has become one of the paradigmatic examples for the transition to turbulence and a large number of bifurcations have been analyzed in considerable detail [2–5]. The limiting case of large radii and fixed gap width where the effects due to curvature become less important and where the system approaches plane Couette flow between parallel walls has received much less attention. In this limit the character of the flow changes: plane Couette flow is linearly stable and the mechanisms that drive the transition to turbulence are still unclear. The question we address here is to what extent the Couette-Taylor system can be used to gain insight into the dynamics of plane Couette flow.

This problem is of both experimental and theoretical interest. As mentioned, the experimental situation for Couette-Taylor flow is much better, there being numerous facilities and detailed studies of patterns, boundary effects and critical parameters [4–6]. The moving boundaries in plane Couette flow reduce the experimental accessibility and the possibilities of applying controlled perturbations. On the theoretical side it is an intriguing question how the change in stability behavior from the Couette Taylor system to the plane Couette system occurs. Studies by Nagata [7] show that some states from the rotating plane Couette system survive the limiting process and appear in finite amplitude saddle node bifurcations in the plane Couette system (see also the investigation of this state by Busse and Clever [8]). Unless the transition from linear instability dominated behavior in Couette-Taylor flow to the shear flow type transition in plane Couette flow is singularly connected to the absence of any curvature it can be expected to happen at a finite radius ratio near which interesting dynamical behavior should occur.

We should mention that there are other useful embeddings of plane Couette. Busse and Clever [8] start from a layer of fluid heated from below with cross flow and proceed to study the stability and parameter dependence of the states. And Cherhabili and Ehrenstein [9] start from plane Poiseuille flow and find localized solutions, albeit at Reynolds numbers higher than the ones studied here.

Our aim here is to follow some of the instabilities in the Couette-Taylor system to the limit of the plane Couette sys-

tem and to identify the parameters where the change in behavior occurs. In particular, we study the transition from laminar Couette flow to Taylor vortices and the instability of vortices to the formation of wavy vortices. Note that the asymptotic situation of plane Couette flow can be characterized by a single parameter, a Reynolds number based on the velocity difference, whereas Couette Taylor flow has at least two parameters, the Reynolds numbers based on the velocities of the cylinders. This extra degree of freedom provides an additional parameter that can be used to modify the flow without changing the basic features.

In cylindrical coordinates (r, ϕ, z) the equations of motion for the velocity components (u_r, u_ϕ, u_z) can be written as

$$\begin{aligned} \partial_t u_r + (\mathbf{u} \cdot \tilde{\nabla}) u_r - \nu \tilde{\Delta} u_r + \partial_r p \\ = \nu \left(\frac{1}{r} \partial_r u_r - \frac{2}{r^2} \partial_\phi u_\phi - \frac{1}{r^2} u_r \right) + \frac{1}{r} u_\phi^2, \end{aligned} \quad (1)$$

$$\begin{aligned} \partial_t u_\phi + (\mathbf{u} \cdot \tilde{\nabla}) u_\phi - \nu \tilde{\Delta} u_\phi + \frac{1}{r} \partial_\phi p \\ = \nu \left(\frac{1}{r} \partial_r u_\phi + \frac{2}{r^2} \partial_\phi u_r - \frac{1}{r^2} u_\phi \right) - \frac{1}{r} u_r u_\phi, \end{aligned} \quad (2)$$

$$\partial_t u_z + (\mathbf{u} \cdot \tilde{\nabla}) u_z - \nu \tilde{\Delta} u_z + \partial_z p = \nu \frac{1}{r} \partial_r u_z, \quad (3)$$

$$\tilde{\nabla} \cdot \mathbf{u} = -\frac{1}{r} u_r, \quad (4)$$

where the modified Nabla and Laplace operators are

$$\tilde{\nabla} = \mathbf{e}_r \partial_r + \mathbf{e}_\phi \frac{1}{r} \partial_\phi + \mathbf{e}_z \partial_z, \quad (5)$$

$$\tilde{\Delta} = \partial_{rr} + \frac{1}{r^2} \partial_\phi \partial_\phi + \partial_{zz}, \quad (6)$$

and where \mathbf{e}_i are the unit basis vectors [10].

The terms in Eqs. (1)–(4) are arranged so that all the ones on the right hand side vanish when the system approaches the plane Couette system, i.e., in the limit of large radii but

finite velocities at the cylinders. The remaining ones become the equations of motion for plane Couette flow in cartesian coordinates (x, y, z) if the identification $x=r$ and $y=\phi r$ is made. However, there are other ways of taking the limit of a small gap that lead to different limiting systems. For instance, the case of almost corotating cylinders with high mean rotation rate gives rise to plane Couette flow with an additional Coriolis term (“rotating plane Couette flow” [7]). Another limit corresponds to the case of counterrotating cylinders with diverging rotation rates [11]. In our numerical work we use the full equations, without any reduction in terms. This allows us to extend Nagata’s work from the rotating plane Couette flow to the full Couette-Taylor system.

The velocities at the inner and outer cylinder (distinguished by indices i and o , respectively) are prescribed and define the boundary conditions

$$u_\phi(r=R_x) = \Omega_x R_x, \quad (7)$$

$$u_r(r=R_x) = u_z(r=R_x) = 0, \quad x = i, o. \quad (8)$$

For the choice of dimensionless quantities we appeal to the plane Couette flow limit. There the relevant quantities are the velocity difference between the walls, $\Delta U = R_i \Omega_i - R_o \Omega_o$, and the gap width $d = R_o - R_i$. Without loss of generality we can always assume $\Omega_i \geq 0$. The Reynolds number for plane Couette flow is based on half the velocity difference and half the gap width,

$$\text{Re} = \frac{\Delta U d}{4\nu}. \quad (9)$$

For the Couette Taylor system there are two Reynolds numbers based on the gap width and the rotation rates of the inner and outer cylinders,

$$\text{Re}_x = R_x \Omega_x d / \nu, \quad (10)$$

where the index x can stand for i or o , the inner and outer cylinders. The plane Couette flow Reynolds number thus is $\text{Re} = (\text{Re}_i - \text{Re}_o)/4$. The ratio of these Reynolds numbers will be called

$$\tilde{\mu} = \text{Re}_o / \text{Re}_i \quad (11)$$

(the tilde is used to distinguish it from $\mu = \Omega_o / \Omega_i$, a frequently defined quantity not used here).

$$\eta = R_i / R_o \quad (12)$$

denotes that ratio of radii.

Experiments and numerical simulations show that plane Couette flow undergoes a subcritical transition to turbulence around $\text{Re}_{PCF} \approx 320$ [12–14]. The Couette-Taylor system shows a first linear instability to the formation of vortices (Taylor-vortex flow, TVF) at Reynolds numbers that depend on the rotation rates and the curvature of the cylinders. In order to see shear flow dominated dynamics the critical Reynolds number for the linear instability has to be above Re_{PCF} . The formation of TVF occurs at Reynolds numbers that can be parametrized in the form

$$\text{Re} = A(\tilde{\mu})(1 - \eta)^{-1/2} + B(\tilde{\mu}) \quad (13)$$

TABLE I. Parameters connected with the Couette-Taylor system in the limit of large radii. A and B are the coefficients in the parametrization (13) of the primary instability. η_{320} is the radius ratio where the primary instability lies above $\text{Re} = 320$; finally, η_c and Re_c are the parameter values for the crossing of the stability curves for Taylor vortex flow and wavy vortex flow.

$\tilde{\mu}$	A	B	η_{320}	η_c	Re_c
0.0	10.8	0.5	0.999	0.990	109
-0.4142	16.8	0.8	0.997	0.977	110
-1.0	33.9	3.2	0.989	0.929	131
-2.4142	53.6	4.6	0.971	≈ 0.94	≈ 220

for $\eta \leq 1$ [15]. This number is larger than the transitional Reynolds number for plane Couette flow if η is sufficiently close to 1. The minimal radius ratio η_{320} where the linear instability occurs for $\text{Re} > 320$ strongly depends on the ratio of the Reynolds numbers of inner and outer cylinder. A few examples for minimal radius ratios η_{320} are summarized in Table I.

Very important for the transition to turbulence in linearly stable systems are nonlinear processes that could give rise to some finite amplitude states, perhaps stationary or periodic, around which the turbulent state could form. One candidate that could serve as a nucleus for turbulence in plane Couette flow is the stationary state first calculated by Nagata [7]. He observed that the wavy vortices that form in a secondary instability from the TVF in the rotating plane Couette system can be followed to the limit of the plane Couette flow where they become part of a saddle node bifurcation at finite Reynolds numbers. This state was also identified and studied in a different limiting process by Busse and Clever [8]. They found that the critical axial and azimuthal wavelengths for this state are

$$\lambda_z = \pi \quad \text{and} \quad \lambda_\phi = 2\pi. \quad (14)$$

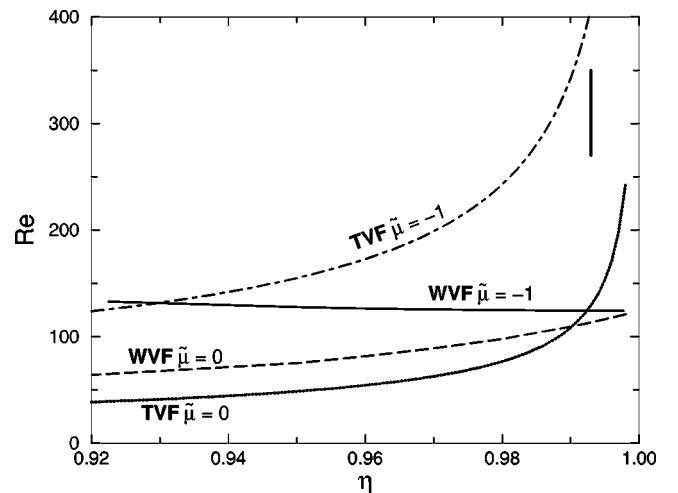


FIG. 1. Bifurcations to Taylor vortex flow (TVF) and wavy vortex flow (WVF) in Couette-Taylor flow for the outer cylinder at rest ($\tilde{\mu} = 0$) and counter-rotating cylinders ($\tilde{\mu} = -1$). The vertical line indicates the parameter range of the lifetime measurements of Fig. 5 at $\tilde{\mu} = -1$.

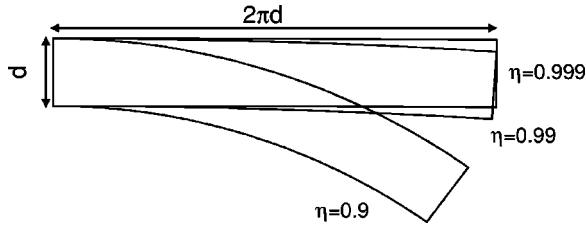


FIG. 2. Geometrical curvature of the cylinders in the Couette-Taylor flow and the plane Couette flow limit. Shown is one fundamental azimuthal wavelength for different radius ratios η as indicated.

This is roughly twice the critical wavelengths that would be expected for Taylor vortices.

We developed a numerical code for the solution of the full Navier-Stokes equation using Fourier modes in axial and azimuthal direction and Legendre collocation in the radial direction. The pressure terms were treated by a Lagrange method. The period in z and ϕ was determined by the fundamental wavelengths (14) of wavy vortex flow.

The continuation of the wavy vortex flow from the Couette-Taylor system to the plane Couette system is shown in Fig. 1 for the case of the outer cylinder at rest ($\tilde{\mu} = 0$) and for counterrotating cylinders with $\tilde{\mu} = -1$. For small η the wavy vortex develops from a secondary bifurcation of TVF, but for sufficiently large η the wavy vortex state is created first in a saddle node bifurcation. The critical Reynolds number for the formation of Taylor vortices diverges as η approaches 1, but the one for the formation of wavy vortices approaches a finite value. Thus the gap in Reynolds numbers between the two transitions widens and the region where plane Couette flowlike behavior can be expected increases with η approaching one. The radius ratios η_c and Reynolds numbers Re_c of the codimension two point where the instabilities for TVF and wavy vortex flow cross are listed in Table I. The ratio of radii η_c where the linear instability of

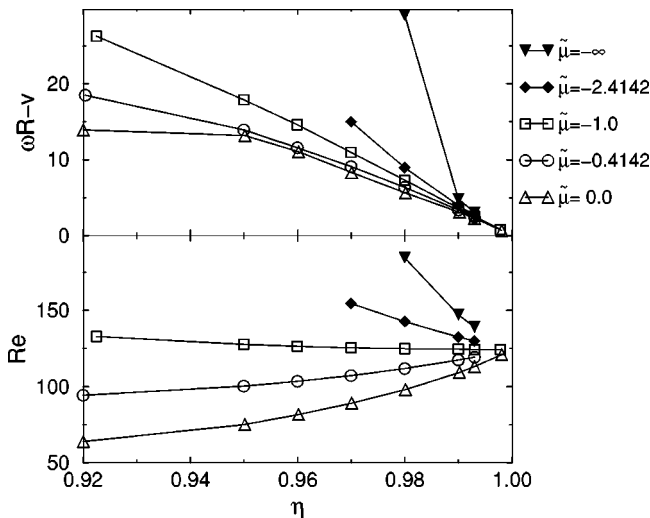


FIG. 3. The convergence to the Nagata-Busse-Clever state for different rotation ratios $\tilde{\mu}$. In the limit of η going to one the wavy vortex states for all $\tilde{\mu}$ approach the same flow that moves with the mean velocity azimuthally. The top diagram shows the rotation speed and the bottom one the critical Reynolds numbers.

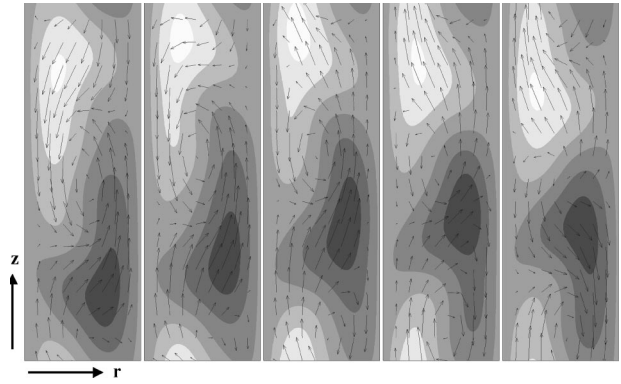


FIG. 4. The wavy vortex flow state near the Nagata-Busse-Clever state at $\eta = 0.993$, $\tilde{\mu} = -1$ and $Re = 124$. Shown is only the disturbance, without the Couette profile. The frames from left to right show cuts through the (r, z) plane at azimuthal wave lengths $\phi = 0, \pi/4, \pi/2, 3\pi/4$ and π . The vectors indicate the r and z components of the velocity field and shading the ϕ component. The inner (outer) cylinder is located at the left (right) side of each frame.

Couette flow and of the Taylor vortex flow cross is a non-monotonic function of the ratio $\tilde{\mu}$ of rotation speed. Both the critical Reynolds numbers for the linear instability of the Couette profile and for the formation of wavy vortices increase with decreasing $\tilde{\mu}$, but at different rates and with different dependencies of η . As a consequence there seems to be a local minimum near about 0.93 for $\tilde{\mu}$ close to -1 .

For the parameter value considered here the curvature of the cylinder walls is geometrically small (see Fig. 2). On the length of one unit cell in ϕ direction the relative displacement in radial direction from a planar wall is about $\pi(1 - \eta)$, i.e., only 3% for $\eta = 0.99$.

The critical Reynolds number for the formation of wavy vortex flow (WVF) seems to converge to the same value for both ratios $\tilde{\mu}$ shown in Fig. 1. The critical Reynolds number as well as the rotation speed of the wavy vortices for several different ratios $\tilde{\mu}$ are collected in Fig. 3. The rotation speed is defined as the angular phase velocity ω of WVF times the

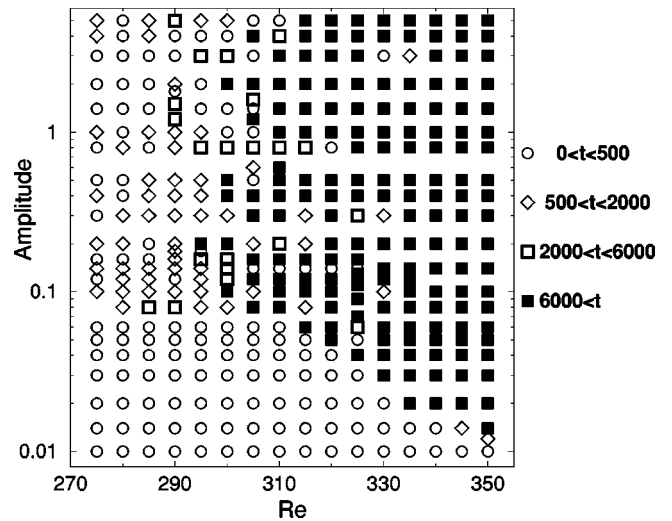


FIG. 5. Lifetime distribution in Couette-Taylor flow at $\eta = 0.993$, $\tilde{\mu} = -1$, and for the indicated range of Reynolds numbers.

mean radius $R = (R_i + R_o)/2$ minus the mean azimuthal velocity $v = (\omega_i R_i + \omega_o R_o)/2$. For all ratios between the speed of inner and outer cylinder the critical Reynolds number for the formation of the wavy vortex state converges to a value of about 125 and the speed of rotation goes to zero. The limiting state that is approached is the stationary Nagata-Busse-Clever state. The velocity field of a wavy vortex solution at $\eta = 0.993$, $\tilde{\mu} = -1$ and $Re = 124$ is shown in Fig. 4; it differs little from the corresponding plane Couette state obtained by Busse and Clever [8], both in appearance and in critical Reynolds number.

In the region above the wavy vortex instability but below the linear instability the dynamics of perturbations shows the fractal lifetime pictures familiar from plane Couette flow [16]. Figure 5 shows an example at a radius ratio of $\eta = 0.993$ and a Reynolds number ratio of $\tilde{\mu} = -1$. The initial state was prepared by rescaling a WVF field obtained at very low radius ratio and Reynolds number. It is interesting to note that even with this initial condition, which is at least topologically close to the Nagata-Busse-Clever state, it is not possible to realize a turbulent signal in its neighborhood: the state quickly leaves this region in phase space. One might have hoped that in spite of the linear instability of the Nagata-Busse-Clever state other states created out of second-

ary bifurcations could have supported some turbulent dynamics in its neighborhood, but the numerical experiments do not support this. The gap between the Reynolds number where the WVF state is formed and the one where typical initial conditions become turbulent is about the same as in plane Couette flow: the WVF states forms around $Re = 125$ and the transition to turbulence, based on the requirement that half of all perturbations induce a long living turbulent state, occurs near a value of $Re_{trans} = 310$, very much as in plane Couette flow [14].

In summary, we have identified parameter ranges in the Couette-Taylor system where some of the characteristics of the plane Couette system can be found. These parameter ranges include radius ratios that can be realized experimentally. Investigations in this regime should be rewarding as they open up the possibility to study the properties of the transition in a closed geometry and to switch continuously between supercritical and subcritical transition to turbulence. The observation of a codimension two point where the linear instability to TVF and the secondary instability to wavy vortex flow cross should provide a starting point for further modeling of the transition in terms of amplitude equations.

This work was financially supported by the Deutsche Forschungsgemeinschaft.

-
- [1] G. I. Taylor, *Philos. Trans. R. Soc. London, Ser. A* **223**, 289 (1923).
- [2] H. A. Snyder, *Int. J. Non-Linear Mech.* **5**, 659 (1970).
- [3] P. S. Marcus, *J. Fluid Mech.* **146**, 65 (1984).
- [4] C. D. Andereck, S. S. Liu, and H. L. Swinney, *J. Fluid Mech.* **164**, 155 (1986).
- [5] R. Tagg, *Nonlinear Sci. Today* **4**, 1 (1994).
- [6] L. Koschmieder, *Bénard Cells and Taylor Vortices* (Cambridge University Press, Cambridge, 1993).
- [7] M. Nagata, *J. Fluid Mech.* **217**, 519 (1990).
- [8] R. M. Clever and F. H. Busse, *J. Fluid Mech.* **344**, 137 (1997).
- [9] A. Cherhabili and U. Ehrenstein, *J. Fluid Mech.* **342**, 159 (1997).
- [10] L. D. Landau and E. M. Lifshitz, *Fluid Mechanics*, 2nd ed. (Pergamon Press, New York, 1987).
- [11] Y. Demay, G. Iooss, and P. Laure, *Eur. J. Mech. B/Fluids* **11**, 621 (1992).
- [12] N. Tillmark and P. H. Alfredsson, *J. Fluid Mech.* **235**, 89 (1992).
- [13] S. Bottin, O. Dauchot, and F. Daviaud, *Phys. Rev. Lett.* **79**, 4377 (1997).
- [14] A. Schmiegél and B. Eckhardt (unpublished).
- [15] A. Esser and S. Grossmann, *Phys. Fluids* **8**, 1814 (1996).
- [16] A. Schmiegél and B. Eckhardt, *Phys. Rev. Lett.* **79**, 5250 (1997).